Title

Selection of DNA nanoparticles with preferential binding to aggregated protein target

Journal

Nucleic Acids Research, 44(10)

ISSN

0305-1048

Authors

Ruff, Laura E

Sapre, Ajay A

Plaut, Justin S

et al.

Publication Date

2016-06-02

DOI

10.1093/nar/gkw136

Published online 11 March 2016

Nucleic Acids Research, 2016, Vol. 44, No. 10 ***e96***
doi: 10.1093/nar/gkw136

Selection of DNA nanoparticles with preferential binding to aggregated protein target

Laura E. Ruff[1,*], Ajay A. Sapre[2], Justin S. Plaut[2], Elisabeth De Maere[3], Charlotte Mortier[3], Valerie Nguyen[1], Kevin Separa[1], Sofie Vandenbogaerde[3], Laura Vandewalle[3], Sadik C. Esener[4] and Bradley T. Messmer[1,*]

[1]UCSD Moores Cancer Center, University of California San Diego, La Jolla, CA 92093, USA, [2]Department of Bioengineering, University of California San Diego, La Jolla, CA 92093, USA, [3]Department Vesalius, Hogeschool Ghent, Ghent 9000, Belgium and [4]Department of Nanoengineering, University of California San Diego, La Jolla, CA 92093, USA

Received November 23, 2015; Revised February 22, 2016; Accepted February 24, 2016

ABSTRACT

High affinity and specificity are considered essential for affinity reagents and molecularly-targeted therapeutics, such as monoclonal antibodies. However, life's own molecular and cellular machinery consists of lower affinity, highly multivalent interactions that are metastable, but easily reversible or displaceable. With this inspiration, we have developed a DNA-based reagent platform that uses massive avidity to achieve stable, but reversible specific recognition of polyvalent targets. We have previously selected these DNA reagents, termed DeNAno, against various cells and now we demonstrate that DeNAno specific for protein targets can also be selected. DeNAno were selected against streptavidin-, rituximab- and bevacizumab-coated beads. Binding was stable for weeks and unaffected by the presence of soluble target proteins, yet readily competed by natural or synthetic ligands of the target proteins. Thus DeNAno particles are a novel biomolecular recognition agent whose orthogonal use of avidity over affinity results in uniquely stable yet reversible binding interactions.

INTRODUCTION

DeNAno DNA particles are a novel multivalent reagent that relies on high overall avidity instead of high affinity to bind their targets. DeNAno particles that specifically bind to primary human dendritic cells (1) and the mouse pancreatic cancer cell line Panc-02 (2) have been selected previously. The selection process is a biopanning strategy akin to that used in aptamer selection by systemic evolution of ligands by exponential enrichment (SELEX), in which a highly diverse library of DNA particles is incubated with the target to capture binders followed by amplification and iteration of the process. While aptamers are generally small pieces of DNA or RNA (<100 bp) that bind in a monovalent fashion with high affinity, DeNAno are concatemers of up to several hundred copies in length made by rolling circle amplification (RCA), with sizes that can be several hundred nanometers (2). This long strand of DNA forms secondary and tertiary structure, which is the basis for ability to bind their targets specifically. In general, folding of ssDNA is dependent on conditions such as temperature, buffer conditions, base-pairing and electrostatic interactions. As with aptamers, DeNAno selection does not require prior knowledge of the target, thus selection on complex targets such as cells is possible. Aptamers have been multimerized via RCA (3), standard nucleic acid chemistry (4) or attachment to nanoparticles (5,6). However, aptamers are—by definition—high affinity, and particles selected in the multivalent format of DeNAno may bind in a different fashion than these multimerized aptamers, leading to identification of different types of binding molecules. Specifically, a DeNAno particle may have many low, monovalent affinity interactions that equal a high overall avidity or the DeNAno may require a minimum copy number to produce the 3D structure required for binding.

The selection process for aptamers and DeNAno is similar. Briefly, in SELEX, a library of 10^{12}–10^{15} oligonucleotides (DNA or RNA) is incubated with a target, washed or otherwise purified, and re-amplified via defined primer sites at the 5′ and 3′ ends of the aptamer. The random region of the aptamer is generally 60–80 bp in length. This process is repeated until binding clones dominate the pool (7,8). The selected aptamers are cloned, sequenced and analyzed, and a binding motif is often identified. These aptamers can have nM-pM affinity, similar to an antibody. Aptamers have been shown to bind via the 3D structure of their primary sequence through a combination of van der Waals forces, hy-

*To whom correspondence should be addressed. Tel: +1 858 534 1783; Fax: +1 858 822 6333; Email: bmessmer@ucsd.edu
Correspondence may also be addressed to Laura E. Ruff. Tel: +1 858 822 0679; Fax +1 858 822 6333; Email: lruff@ucsd.edu

drogen bonding, salt bridges, hydrophobic interactions and electrostatic interactions (9,10). Selection of DeNAno particles occurs in a similar fashion. DeNAno are made via RCA of circularized oligonucleotide templates containing random regions of sequence. The resulting DeNAno is a concatemer of single-stranded DNA with sequence complementary to the circularized oligonucleotide template. 10^{10}–10^{11} particles are incubated with a target, washed and re-amplified via defined primer sites at the 5′ and 3′ ends of the oligonucleotide template. The template strand is enriched via asymmetric polymerase chain reaction (PCR), circularized and the selection process is repeated until binding particles dominate the pool. As with aptamers, DeNAno with primary sequence motifs have been identified (2).

In this paper, DeNAno particles that bind to specific proteins are identified and characterized. Streptavidin was used as a well-characterized model system and monoclonal antibodies were chosen to confirm these results because of their potential use in biologic assays. Two intriguing phenomena were observed during the course of this study: (i) DeNAno were displaced from their target by the corresponding ligand and this event could be quantitated in multiple ways and (ii) DeNAno preferentially bound aggregated rather than free target. The findings described in this paper set the stage for several novel applications of DeNAno affinity reagents, such as 'wash-free' immunoassays and massively parallel multiplexed assays.

MATERIALS AND METHODS

DeNAno particle synthesis and characterization

DeNAno particles were made by RCA, as previously described (1). Briefly, a 100-bp template oligo (Integrated DNA Technologies; IDT, Coralville, IA, USA, all oligos from IDT unless otherwise specified) was circularized via a 40-bp complementary oligo and ligated with T4 ligase (New England Biolabs; NEB, Ipswich, MA, USA). RCA was then performed on this template, using the complementary oligo as the initiating oligo and phi29 DNA polymerase (NEB). RCA was performed at 30°C for 30 m, with a dNTP concentration of 3 nmol or 93.8 pmol. Enzyme was heat inactivated at 65°C for 10 m or 95°C for 5 m. The resulting DeNAno particles are concatemers complementary to the circularized template. Their size is influenced by the amount of time the reaction is run and the concentration of dNTPs (NEB). For fluorescent readouts, particles were labeled with 1/10 molar ratio Alexa Fluor 647-labeled complementary oligo. For streptavidin experiments, positive control particles were made by labeling particles with 1/10 molar ratio 5′ biotinylated complementary oligo (see Supplementary Table S1 for oligo sequences).

Beads

Streptavidin-coated magnetic beads (NEB) were used for selections/staining for streptavidin-specific DeNAno with no modifications. For rituximab and bevacizumab selections/staining, coated beads were made as follows: 6 μm polystyrene beads (Polysciences, Warrington, PA, USA) were washed with 20 mM sodium phosphate buffer pH 7.5 (Boston BioProducts, Ashland, MA, USA), then coated with 100 μg/ml rituximab (Genentech, South San Francisco, CA, USA), bevacizumab (Genentech), or polyclonal human IgG (Thermo Fisher Scientific, Waltham, MA, USA) diluted in 20 mM sodium phosphate pH 7.5. Beads and antibody were incubated for 2 h at room temperature (RT) or overnight at 4°C. Non-adsorbed antibody was removed with 3 × 1 ml washes with 20 mM sodium phosphate pH 7.5. Finally, beads were resuspended in phosphate bufferedsaline (PBS) (without calcium and magnesium, Mediatech, Manassas, VA, USA) supplemented with 0.02% NaN_3 (Ricca Chemical Company, Arlington, TX, USA).

In one control experiment, streptavidin polymethyl methacrylate (PMMA) (Sapidyne Instruments, Boise, ID, USA) and streptavidin sepharose (GE Healthcare Life Sciences, Piscataway, NJ, USA) were used in place of streptavidin magnetic beads.

DeNAno selections

DeNAno selections were performed as previously described, with minor modifications (1). For the streptavidin and rituximab selections, 3×10^{10} nanoparticles were incubated with target beads for 20 m at RT. For streptavidin, the target was streptavidin-coated magnetic beads; for rituximab selections, the target was rituximab-coated beads (described above). Non-binding particles were removed by repeated washes. Bound DeNAno particles were amplified by Hemo KlenTaq (NEB) back to the 100-bp oligo, and the template strand was amplified by asymmetric PCR. The template strand was then re-circularized as above and the entire process repeated through 4–5 rounds of selection. 100-bp oligos were then cloned into pGEM T-easy vector (Promega, Madison, WI, USA), transformed into NEB 5-alpha high efficiency competent cells (NEB) and sequenced via colony PCR (Eton Bioscience Inc, San Diego, CA, USA).

Selection on bevacizumab-coated beads differed in these ways: round one selection was performed with 10 times more particles (3×10^{11} unique particles) and selection was performed overnight at 4°C. Subsequent selection rounds were performed for 2–4 h at RT, but with a standard number of DeNAno particles (3×10^{10}). These conditions were employed because multiple selection attempts with the standard conditions failed.

DeNAno staining

For initial experiments, clones of selected particles were generated via PCR of the pGEM T-easy insert, followed by asymmetric PCR to amplify the template strand. Circularization and RCA were then performed, as above. RCA conditions were 30°C for 30 m with 3 nmol dNTP, followed by heat inactivation for 10 m at 65°C—these are the standard RCA conditions used, unless otherwise noted. Templates for clones of interest were synthesized (IDT).

All stainings were performed in a pre-blocked 96-well v-bottom plate. Pre-block was PBS 1% bovine serum albumin (BSA) (Sigma, St Louis, MO, USA) supplemented with 10 mM $MgCl_2$ (Teknova, Hollister, CA, USA; PBS 1% BSA 10 mM $MgCl_2$). Unless otherwise noted, ∼3 ×

10^{10} fluorescently-labeled particles were incubated with 2 μl coated beads for 20 m at RT in PBS 10 mM $MgCl_2$. Beads were then washed once with PBS 10 mM $MgCl_2$, twice by Tris-buffered saline (Mediatech) 0.05% Tween-20 (Thermo Fisher Scientific) 10 mM $MgCl_2$ (TBST 10 mM $MgCl_2$), once with PBS 10 mM $MgCl_2$ and resuspended in PBS 10 mM $MgCl_2$. Washes were performed by magnetic pulldown (streptavidin beads) or centrifugation at 1000 × *g* for 3 m (rituximab and bevacizumab beads). Fluorescence was measured with a multimode microplate reader (TECAN, Männedorf, Switzerland).

Transmission electron microscopy

All transmission electron microscopy (TEM) Images were taken on a FEI Technai G^2 Sphera transmission electron microscope (FEI, Hillsboro, OR, USA) operating at 200 kV. Copper grids (formvar/carbon-coated, 400 mesh copper, Ted Pella, Inc., Redding, CA, USA) were prepared by glow discharging the surface at 20 mA for 1.5 m followed by treatment with 20 μl 100 mM $MgCl_2$ for 1 m in order to prepare the surface for DNA nanoparticle adhesion. The solution was wicked away and 4 μl of DeNAno sample was deposited on the grid and allowed to sit for 30 s. All grids were treated with three drops of 1% w/w uranyl acetate (Mallinckrodt, Dublin, Ireland) to provide negative staining. DeNAno particles were dialyzed into 10 mM Tris 10 mM $MgCl_2$ pH8.5 prior to imaging and loading on the grid, using a slide-a-lyzer 10K MWCO dialysis cassette (Thermo Fisher Scientific).

Atomic force microscopy

Samples were prepared on freshly cleaved muscovite mica (Ted Pella, Inc.). Mica disks were nicked with a scalpel and vacuum cleaved then coated with a 0.005% w/v aqueous solution of poly-L-lysine (PLL, MW 30–70 kDa, Sigma), rinsed with deionized water, and dried overnight in a dessicator. Dialyzed SA-D8 particles (prepared as in TEM) were adsorbed to the PLL-mica for 30 m, rinsed with deionized water and dried in a dessicator until imaged.

Images were acquired using ScanAsyst Si3N4 probes (Al-coated, 0.4 N/m spring constant, Bruker, Billerica, MA, USA) with PeakForce Tapping Mode on a MultiMode 8 atomic force microscope (NanoScope V Controller, Bruker).

dNTP dilution experiment

For dNTP dilution experiment, standard particles were made—30 m/30°C/3 nmol dNTP, as well as 30 m/30°C/93.8 pmol dNTP. These particles were all heat inactivated at 95°C for 5 m. Control particles from another library (V10control) with the same conditions were also made and used as an internal control in the staining. Unlabeled DeNAno particles were mixed with the internal control particles of the same size/condition and incubated with 8 μg streptavidin beads for 2.5 h at RT in PBS 1% BSA 10 mM $MgCl_2$. Samples were resuspended and an aliquot was taken before proceeding to the wash step. Beads were then washed via magnetic pulldown, once with PBS 1% BSA 10 mM $MgCl_2$, three times with TBST 1% BSA 10 mM $MgCl_2$, once with PBS 1% BSA 10 mM $MgCl_2$ and resuspended in PBS 1% BSA 10 mM $MgCl_2$. Bound and total samples were analyzed by qPCR. A standard was run for each library (a plasmid containing the 100bp template used to make DeNAno). The ratio of the bound particles (streptavidin DeNAno:control DeNano) to total particles (streptavidin DeNAno:control DeNAno) is graphed.

Competitive titration experiment

For competitive titration experiments, biotin (K_d ~10^{-15} M), *d*-desthiobiotin (K_d ~10^{-11} M) or 2-iminobiotin (K_d ~10^{-8} M at pH7.5; all from Sigma) were pre-incubated with streptavidin beads for 20 m in DPBS (with calcium and magnesium; Mediatech) 1% fetal bovine serum (FBS; Omega Scientific, Tarzana, CA, USA) or rituximab-specific peptide or irrelevant peptide were pre-incubated with rituximab beads for 20 m in PBS 10 mM $MgCl_2$. Fluorescently-labeled particles were then added and allowed to incubate for a further 20 m. Washes were performed via magnetic pulldown for streptavidin beads or centrifugation at 1000 × *g* for 3 m for rituximab beads. A biotinylated particle was used as a positive control for streptavidin experiment.

For streptavidin competitive titration experiment, free streptavidin was pre-incubated with fluorescently-labeled DeNAno for 20 m in DPBS 1% FBS, followed by addition of streptavidin magnetic beads for a further 20 m. Washes were performed via magnetic pulldown. A biotinylated particle was used as a positive control.

Competitive release experiment

For biotin and streptavidin competitive release experiments, fluorescently-labeled particles were pre-incubated with streptavidin beads in DPBS 1% FBS for 20 m at RT. Biotin, *d*-desthiobiotin, 2-iminobiotin or streptavidin (ProSpec, East Brunswich, NJ, USA) were then added and incubated for an additional 20 m. Washes were performed as above. A biotinylated particle was used as a positive control.

For rituximab/peptide competitive release experiments, particles were pre-incubated with rituximab beads in PBS 10 mM $MgCl_2$ for 20 m at RT. A total of 50 μg/ml rituximab peptide, irrelevant peptide or buffer were then added and incubated for an additional 1 h. An aliquot of this total sample was taken, then the beads were spun down at 1000 × *g* for 3 m and the supernatant was collected. The supernatant was spun down an additional two times to ensure that all beads were removed from the sample. DeNAno content of total and supernatant samples was then measured by qPCR, using a plasmid containing 100-bp oligo from the same library as a standard. % release was measured as supernatant DeNAno/total DeNAno * 100%.

DeNAno dissociation experiment

For dissociation experiment, standard conditions were used to make DeNAno particles. Unlabeled DeNAno particles were incubated with 8 μg streptavidin beads for 2.5 h at RT in PBS 1% BSA 10 mM $MgCl_2$ and washed as in the

dNTP dilution experiment. Samples were then resuspended in 10 ml PBS 1% BSA 10 mM $MgCl_2$ and stored at 4°C. At days 1, 8, 14, 21, 28 and 35 aliquots of total sample (beads + supernatant) and supernatant-only were taken. To acquire supernatant-only, 100 μl of total sample was incubated on a magnet for 5 m to remove beads from sample. Supernatant was removed to a new well and the procedure was repeated twice more. Total and dissociated samples were analyzed by qPCR and quantitated with a standard for that library. Percentage released DeNAno is graphed (dissociated/total*100%).

Rituximab-binding peptide

Rituximab-binding peptide sequence and irrelevant peptide sequence was ordered from (Genscript, Piscataway, NJ, USA). The rituximab-binding peptide has been shown to bind at the antigen-binding site of rituximab and compete with target cell surface receptor for mAb binding. The K_d of surface immobilized peptide-whole antibody was reported to be 131 nM and 3.99 μM for surface immobilized peptide-Fab fragment (11) Peptide was used in place of recombinant CD20 due to the amount required for titration and release experiments.

Protein G sandwich assay

For protein G sandwich assay, fluorescently-labeled rituximab-specific, bevacizumab-specific or library negative DeNAno particles or anti-human kappa light chain antibody (clone HP6062; Thermo Fisher Scientific) were used. Protein G magnetic beads (Thermo Fisher Scientific) were incubated with rituximab or bevacizumab for 1 h at RT in PBS 1% BSA 10 mM $MgCl_2$. For anti-kappa samples only: mouse IgG2b (clone eBM2b; eBioscience, San Diego, CA, USA) was added to rituximab and bevacizumab samples that would be less than saturating (<1-fold on graph) to bind all the protein G so anti-kappa antibody would not bind to these non-specifically. DeNAno particles or anti-human kappa light chain antibody Alexa Fluor 488 (Thermo Fisher Scientific Inc) were then added and incubated for 2 h at RT (no washing step was performed prior to their addition). After incubation, all samples were washed via centrifugation (900 × *g*, 3 m), once with PBS 1% BSA 10 mM $MgCl_2$, three times with TBST 1% BSA 10 mM $MgCl_2$, once with PBS 1% BSA 10 mM $MgCl_2$ and resuspended in PBS 1% BSA 10 mM $MgCl_2$. Sample fluorescence was read on a multimode microplate reader for both Alexa Fluor 488 (anti-kappa) and Alexa Fluor 647 (DeNAno).

DNA modeling

mFold (The RNA Institute, College of Arts and Sciences, SUNY Albany, NY, USA) was used for DNA modeling. DNA conditions used were: 4°C conditions with 0.15 M Na^+ and 0.01 M Mg^{2+} ionic conditions. Representative structures are shown when the output provided more than one structure. Motif analysis was performed with the MEME suite program (12).

RESULTS

Streptavidin-binding DeNAno

The well-characterized protein streptavidin was the first target chosen to determine if DeNAno particles could be selected against a defined protein. A library of DeNAno particles was made as described in 'Materials and Methods' section and used in a selection on streptavidin-coated magnetic beads as outlined in Figure 1A. All oligonucleotide sequences are listed in Supplementary Table S1 (MJ library and primers). Following five rounds of selection, a population of streptavidin-binding particles emerged, as indicated by a >10-fold increase in fluorescently-labeled DeNAno bound to streptavidin, from library to round five (Figure 1B). The 100-bp core oligo of sixteen round five-selected DeNAno was sequenced. Four sequences were identified, including one dominant clone, SA-D8, which represented 11/16 sequences obtained (Table 1). All clones bound to streptavidin-coated beads, but not BSA-coated beads (Figure 1C). A random clone from the same library was used as a negative control (G10neg) and showed no binding to the beads. This same clone was incubated with a biotinylated complementary oligo and used as a positive control (G10bio). SA-D8 was also tested on streptavidin-coated sepharose and PMMA beads to confirm binding specificity for streptavidin (Supplementary Figure S1A and B). Sequence analysis was performed on these clones using MEME suite program (12) and a motif was identified, ACGACGCA (Supplementary Figure S2A and B). DNA modeling put this motif in part of a stem-loop structure for each of the four clones (Supplementary Figure S2C). Interestingly, similar binding motifs or low-homology motifs with conserved nucleotides in the binding region have been reported for streptavidin-binding aptamers from four other laboratories (13–16). In these cases, the motif was important for aptamer binding to streptavidin, and this binding was inhibited by biotin.

The dominant DeNAno clone, SA-D8, was imaged using atomic force microscopy (AFM; Figure 2A) and TEM (Figure 2B and C, and Supplementary Figure S3A). For TEM, both 'standard' (the size of particle used throughout the paper) and 'small' (used in Figure 2D) particles were made. In all cases, discreet 'balls' of DNA were observed, with a diameter of 100–250 nm (AFM), 75 nm (standard DeNAno/TEM) or, 58 nm (small DeNAno/TEM), similar in size to previous reports using nanoparticle tracking system (Nanosight) (2). The disparity between TEM and AFM size of standard DeNAno is most likely due to the compactness of the imaged DeNAno, which is partly determined by the amount of salt present in the sample and the preparation method. An image of the 'standard' size library particles is also included in Supplementary Figure S3B.

To assess binding capability, standard and small size DeNAno were made by varying dNTP concentration in the RCA reaction. The DeNAno tested were SA-D7, SA-D8, G10neg, G10bio and V10control. V10control is a DeNAno from a different library which was made in two different sizes and mixed with the experimental particles for use as an internal control. DeNAno bound to streptavidin beads and total samples were analyzed by qPCR. A standard was run

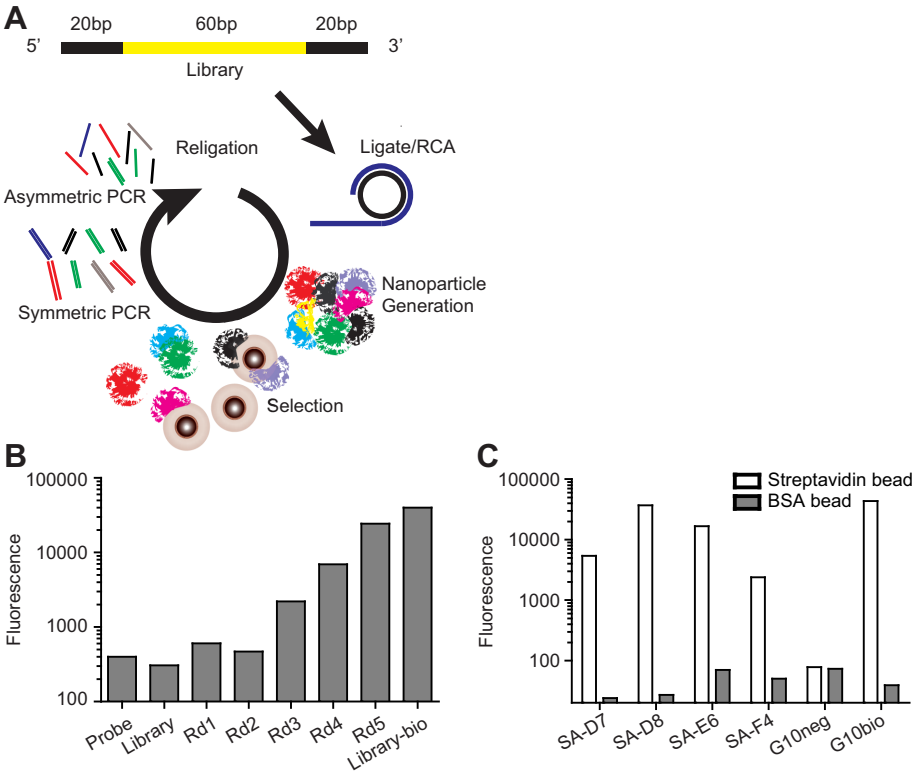

Figure 1. Selection of streptavidin-binding DeNAno. (**A**) Schematic of selection process. (**B**) Staining of streptavidin selection rounds 1–5. Probe-only, library and positive control (biotinylated library) are also shown. (**C**) Staining of four selected streptavidin clones on streptavidin beads and BSA-coated beads. Negative control clone (G10neg) and biotinylated positive control clone (G10bio) also shown.

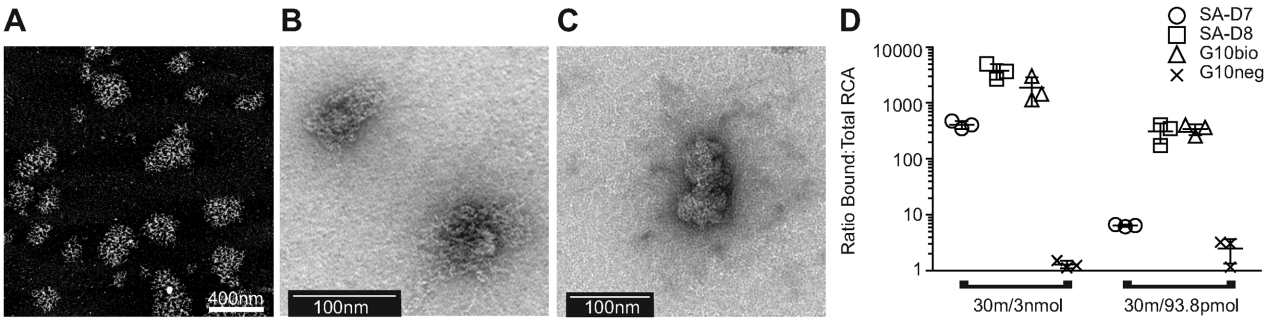

Figure 2. Imaging of DeNAno and staining different size DeNAno. (**A**) Atomic force micrograph (AFM) of dried DeNAno SA-D8 on poly-L-lysine-coated mica. Scale = 400 nm. (**B**) SA-D8 DeNAno roughly 75 nm in diameter as observed by transmission electron microscopy (TEM) using negative staining. Scale = 100 nm. (**C**) TEM of small SA-D8 DeNAno roughly 58 nm in diameter. Scale = 100 nm. (**D**) Binding of streptavidin DeNAno of different sizes made by alteration of dNTP concentration. DeNAno particles were made with 3 nmol dNTPs for 30 m at 30°C (the standard conditions), or 93.8 pmol dNTPs for 30 m at 30°C. A control DeNAno from a different library was also made for both of these conditions and used as an internal control in the staining and subsequent PCR. The ratio of the bound particles (streptavidin DeNAno:control DeNano) to total particles (streptavidin DeNAno:control DeNAno) is graphed.

for each library—10-fold dilutions of a plasmid containing the 100-bp DeNAno template. The ratio of the bound particles to total particles is shown in Figure 2D. At the standard particle size, all particles except G10neg bound to the streptavidin beads, as indicated by their high bound:total ratios. When the particle size was reduced, SA-D7 binding dramatically dropped off and was only slightly above background (G10neg); SA-D8 and G10bio binding were not greatly affected. This result may indicate that SA-D7 DeNAno is more dependent on total avidity than SA-D8 to bind its target. This suggests DeNAno are not simply aptamers made into concatemers by RCA, which has been previously demonstrated (3).

Surface plasmon resonance (SPR) and kinetic exclusion assays (KCA) were unsuccessfully attempted to obtain a K_d value for the DeNAno particles. In the case of SPR, no reading was obtained, perhaps due to the spacing of the target (streptavidin) on the chip, as it is likely that one DeNAno binds multiple streptavidin. For KCA, binding to the streptavidin PMMA beads was observed, however, the binding

Table 1. Streptavidin clones

Clone	Primer	Random region	Primer	#
SA-D7	TGCTTTTTGGAACTCCTGCT	TTGTTTTTCTCTAGTACACTTCACTCGCATTAAAGTCTATACGCAACCGGCACCGACGCA	GGTGACGTTGAGTTGGATCCA	3
SA-D8	TGCTTTTTGGAACTCCTGCT	AGAATATATGACTAGTTTTATATGACACTGTCGAAACGACGCAGTGAGATAGTGATAATT	GGTGACGTTGAGTTGGATCCA	11
SA-E6	TGCTTTTTGGAACTCCTGCT	GATTGGTTACCACACCTTTCATGAATCATGCTTTACGGGCTGCCAAGAACTGAACCTCA	GGTGACGTTGAGTTGGATCCA	1
SA-F4	TGCTTTTTGGAACTCCTGCT	GAACATGCGGGAATGAACGGGAATCAGTCAAAAATACTCAATTAAATCCCATGACGCAAT	GGTGACGTTGAGTTGGATCCA	1

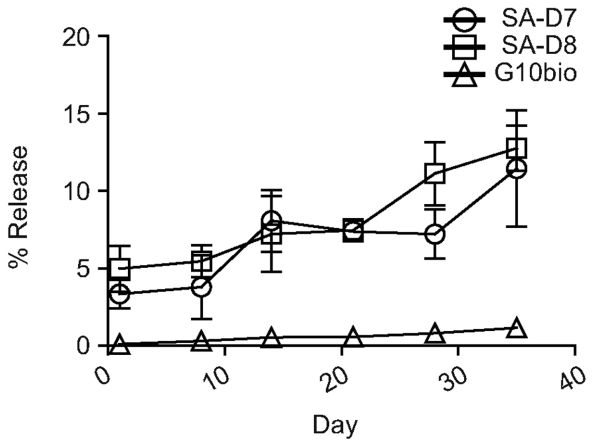

Figure 3. Dissociation of streptavidin-binding DeNAno over time. Streptavidin-coated magnetic beads were stained with DeNAno particles. The stained beads were then incubated in 10 ml buffer for 35 days. Aliquots were taken every week of the total sample (supernatant plus beads) and supernatant only (beads were removed by magnet). PCR was done on all samples/timepoints and percentage release is graphed (DeNAno in supernatant/DeNAno in total * 100%).

could not be inhibited by free streptavidin and thus no value could be obtained (data not shown). Instead, a dissociation time course was performed, using SA-D7, SA-D8 and G10bio (Figure 3). DeNAno were incubated with streptavidin beads, washed extensively and the DeNAno-coated beads were resuspended in 10 ml buffer. Samples were taken weekly through day 35 and either analyzed directly or the beads were pelleted and the supernatant analyzed. DeNAno binding to the streptavidin beads was remarkably durable, with only ∼12% of total particles found in the supernatant at day 35. This dissociation was only 9.9-fold (SA-D7) and 11-fold (SA-D8) above that of G10bio.

SA-D8 was tested for binding in the presence of competitor oligo (Supplementary Figure S4). An excess of 100-bp oligo with the same sequence as the SA-D8 DeNAno was pre-incubated with streptavidin beads, followed by addition of fluorescently-labeled DeNAno. No inhibition of SA-D8 binding was observed in the presence of SA-D8 competitor oligo or irrelevant oligo, suggesting the DeNAno requires multiple copies of the oligo sequence to bind or that the avidity of the DeNAno is sufficiently greater than the affinity of the individual oligos for streptavidin.

To further define the properties of DeNAno, the effect of buffer composition on the binding capacity of the particles was evaluated. SA-D7, SA-D8, G10neg and G10bio were selected for testing. The following conditions were assessed: $MgCl_2$ concentration, NaCl concentration, physiologic buffers and biologic buffers. It is known that cations such as magnesium and sodium can reduce repulsion along the negatively charged backbone of the ssDNA, resulting in particles with more flexibility and shorter effective length (17). Thus, alteration of these cation concentrations may affect the structure of the particle, and thus ability to bind. For $MgCl_2$ concentration, binding was observed in $\geq$5 mM $MgCl_2$, with no adverse effects up to 40 mM $MgCl_2$; no effect on binding was observed for 0–300 mM NaCl (Supplementary Figure S5A and B). Binding was observed in all

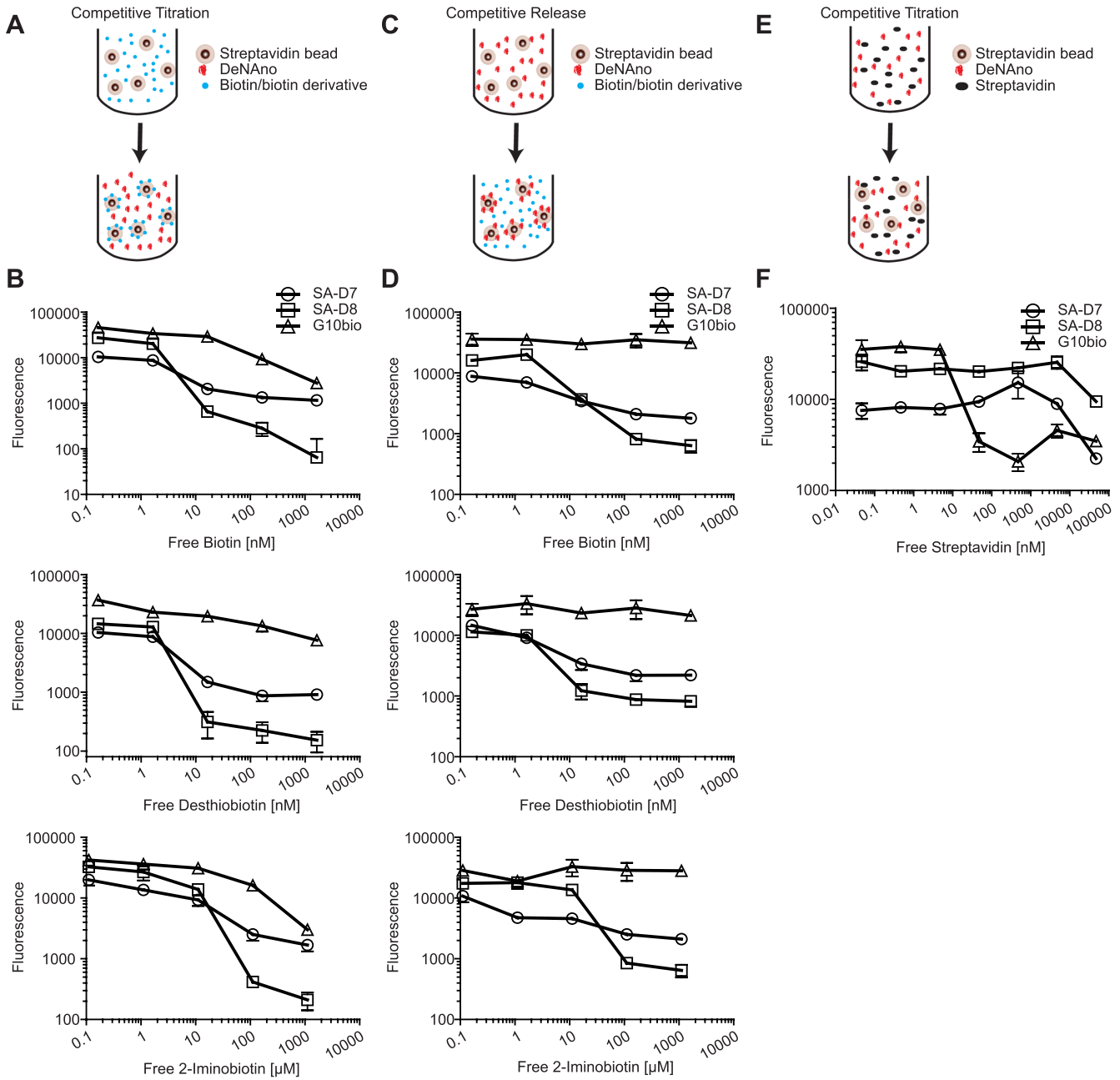

Figure 4. Competitive titration and competitive release of streptavidin-binding DeNAno with biotin/biotin derivatives or streptavidin. (**A**) Schematic of competitive titration using biotin/biotin derivatives. (**B**) Free biotin (top), desthiobiotin (middle) and 2-iminobiotin (bottom) competition titrations were done by pre-incubating streptavidin beads with one of the biotin/biotin derivatives (or buffer for the baseline), then adding DeNAno particles. (**C**) Schematic of competitive release using biotin/biotin derivatives. (**D**) Biotin (top), desthiobiotin (middle) and 2-iminobiotin (bottom) competitive release assays were done by staining streptavidin beads with DeNAno particles, then adding biotin/biotin derivative (or buffer for baseline). (**E**) Schematic of streptavidin competitive titration. (**F**) Free streptavidin competition titration of SA-D7 and SA-D8 clones and G10bio positive control. Fluorescently-labeled DeNAno particles were pre-incubated with varying concentrations of free streptavidin, then streptavidin beads were added.

physiologic buffers tested, with some variability in intensity (Supplementary Table S2 and Supplementary Figure S5C). High levels of fluorescence were observed in MES, HEPES, bicine, CAPSO, carbonate, sodium phosphate, PBS and TBS, and lower fluorescence signal (but still above G10neg signal) was observed in PIPES, citrate and water. Finally, particle binding was tested in 1.1, 3.3, 10 and 30% urine, FBS and human serum (Supplementary Figure S5D). SA-D8 bound streptavidin beads in all conditions except 30% urine, while SA-D7 did not bind in 10% urine or 30% of any biologic buffer. Overall, these results indicate the DeNAno particles bind in a variety of buffers and conditions, and perhaps unsurprising, are suited for the conditions they were selected in—namely 10 mM $MgCl_2$, 150 mM NaCl and tris or sodium phosphate buffer. Additionally, the particles'

ability to bind in biologic buffers demonstrates potential for diagnostic or *in vivo* use.

As streptavidin-specific aptamers have previously been shown to be displaced from their target by biotin, SA-D7, SA-D8, G10neg and G10bio DeNAno were tested for binding to streptavidin in the presence of biotin and biotin derivatives in two assay formats (competitive titration and competitive release, Figure 4A–D). In the competitive titration assay, different concentrations of biotin, desthiobiotin or 2-iminobiotin (pH 7.5) were pre-incubated with streptavidin beads, then fluorescently-labeled DeNAno particles were added, further incubated, washed and fluorescence measured on a multimode microplate reader (Figure 4A and B). All particles were inhibited by high doses of biotin or biotin derivative. In the case of biotin and desthiobiotin, this inhibition occurred slightly below the estimated stoichiometric dose of 1:1 biotin:streptavidin sites (53.3 nM biotin). For 2-iminobiotin, whose K_d decreases with pH, ∼10 000-fold excess was required to completely inhibit DeNAno binding. These same clones were also tested in a competitive release experiment, in which streptavidin beads were pre-incubated with fluorescently-labeled DeNAno particles, followed by addition of biotin, desthiobiotin, or 2-iminobiotin, further incubated, washed and fluorescence measured on a multimode microplate reader (Figure 4C and D). G10bio particle showed no decrease in fluorescence, due to the exceptionally slow dissociation kinetics of biotin-streptavidin. SA-D7 and SA-D8 showed decreased fluorescence for all biotin derivatives at the same concentrations observed for the competitive titration experiment. Thus, these streptavidin-binding DeNAno particles are not only inhibited, but also removed by ligand. Ligand displacement of DeNAno essentially transforms a protein binding event into a DNA signal—a feature that could have use as a high throughput ligand-receptor sensor.

Next, the competitive titration assay was used to directly test whether free streptavidin could inhibit DeNAno binding (Figure 4E and F). Free streptavidin was pre-incubated with fluorescently-labeled DeNAno, followed by addition of streptavidin beads. G10bio performed as expected, exhibiting a sharp decrease in fluorescence at the estimated 1:1 stoichiometric dose. SA-D7 and SA-D8, however, required 100–1000-fold excess streptavidin to induce a decrease in signal. Thus, the DeNAno particles' behavior appears contrary—they are removed/inhibited by free ligand (biotin and derivatives), yet their binding is not inhibited by excess target (streptavidin). In fact, they seem to bind preferentially to aggregated streptavidin (bead) versus free streptavidin. DeNAno particles are therefore unique affinity reagents that bind in the presence of high concentrations of free target and may be particularly useful in assays limited by the 'high-dose hook effect'. This effect is observed most often in lateral flow assays (LFA) or other assays that do not employ an intermediate wash step. When there is an overabundance of target in the assay, the detection and/or capture antibodies are limiting, leading to target that is only bound to one antibody and not both (leading to a false negative) (18–20).

Table 2. Rituximab and bevacizumab clones

Rituximab			
Clone	Primer	Random region	Primer	#
3Rit1	TGCTTTTTGGAACTCCTGCT	GGAGATTAATCTCAAACTTTCAATATGCGTAGCTTATCCGTGTCGTTAAGAACGGCGTCA	GGTGACGTTGAGTTGGATCCA	5
Bevacizumab				
Clone	Primer	Random region	Primer	#
Bev1	TGCTTTTTGGAACTCCTGCT	GTTTCTCAAATGGACTGATCCATGGGTTTTAAGGAAAAATAGAGTGTGTTGTAACAAACT	GGTGACGTTGAGTTGGATCCA	9
Bev8	TGCTTTTTGGAACTCCTGCT	GTTTCTCAAGTGGACTGATCCATGGGTTTTAAGGAAAAATAGAGTGTGTTGTAACAAACT	GGTGACGTTGAGTTGGATCCA	1

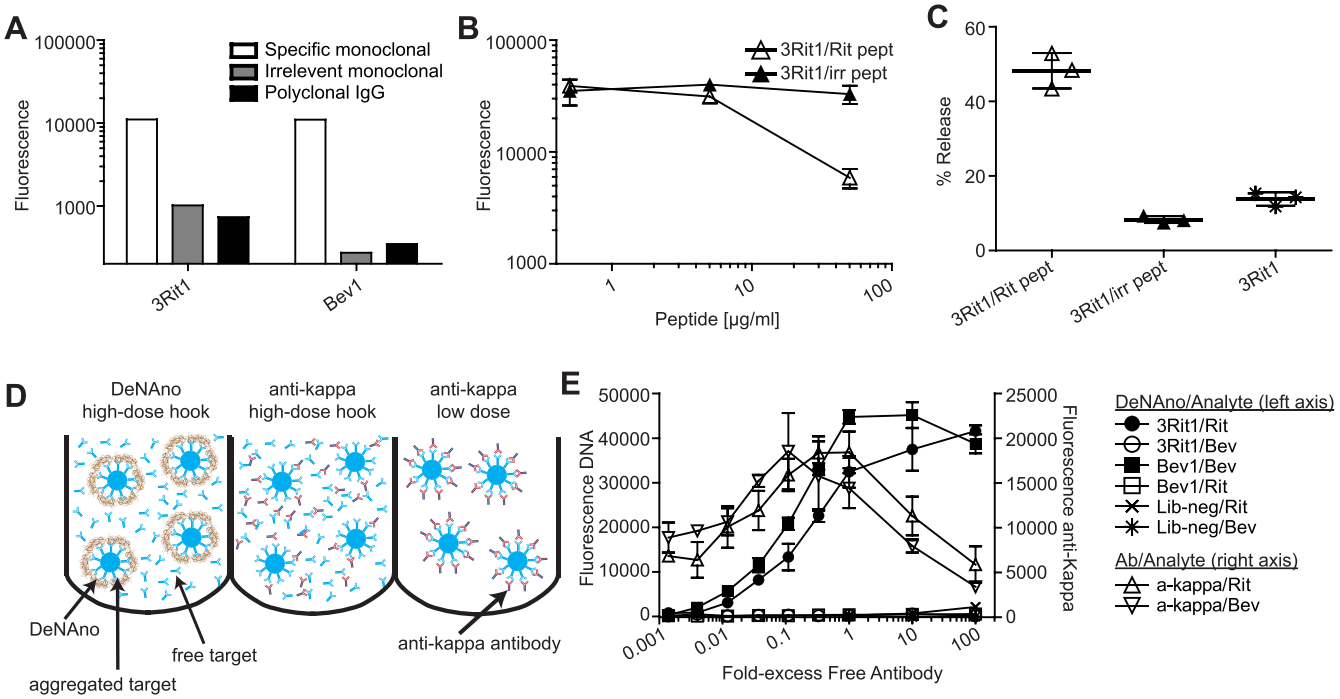

Figure 5. Antibody-specific DeNAno. (**A**) Staining of dominant clones from rituximab (3Rit1) and bevacizumab (Bev1) selections on specific monoclonal-, irrelevant monoclonal- and human polyclonal IgG antibody-coated beads. (**B**) Competitive titration with rituximab-specific (Rit pept) or irrelevant peptide (irr pept) was done by pre-incubating peptide with rituximab-coated polystyrene beads, followed by incubation with fluorescently-labeled3Rit1 DeNAno. (**C**) Competitive release with peptide was done by pre-incubating rituximab-coated polystyrene beads with 3Rit1 DeNAno, followed by incubation with Rit pept, irr pept or buffer. Total sample and sample released into the supernatant were measured by qPCR and percentage released is graphed. (**D**) Schematic of high-dose hook effect experiment for DeNAno in high-dose conditions and anti-kappa in high-dose and low-dose conditions. (**E**) Protein G was pre-incubated for 1 h with different concentrations of rituximab or bevacizumab. Alexa Fluor647-labeled 3Rit1 DeNAno, Bev1 DeNAno or Lib-neg DeNAno (left y axis), or Alexa Fluor488-labeled anti-kappa human light chain antibody (right y axis) were then added and incubated for an additional 2 h, then washed and measured for fluorescence. For anti-kappa light chain samples only: rituximab and bevacizumab samples <1-fold free antibody were diluted with mouse IgG2b κ to equal 1-fold total antibody. This was done to bind all free protein G sites before addition of anti-kappa antibody so it would not bind non-specifically.

Rituximab- and bevacizumab-binding DeNAno

Phage display has previously identified peptides that bind specifically to monoclonal antibodies (11,21,22). The DeNAno selection technique was applied to monoclonal antibody-coated beads to determine if DeNAno specific for monoclonal antibodies could be identified with similar properties to the streptavidin-binding DeNAno. After four rounds, a binding population emerged for both selections and one dominant clone was identified for each (Supplementary Figure S6 and Table 2). The binding of these clones was tested on specific and irrelevant monoclonal antibody-coated beads, as well as polyclonal human IgG-coated beads (Figure 5A). 3Rit1 (rituximab-specific) bound with >10-fold signal above control beads and Bev1 (bevacizumab-specific) bound with >30-fold signal.

Next, competitive titration and competitive release experiments were performed with 3Rit1 DeNAno and a previously-identified rituximab-specific mimetope peptide (11) to determine if these DeNAno could also be used as a ligand-receptor sensor. For the competitive titration, 0–50 μg/ml rituximab peptide or irrelevant peptide was pre-incubated with rituximab-coated beads, followed by addition of fluorescently-labeled 3Rit1 DeNAno. 3Rit1 exhibited a decrease in fluorescence only in the presence of 50 μg/ml rituximab peptide (Figure 5B). In the competitive release experiment, 3Rit1 was pre-incubated with rituximab-coated beads, followed by addition of 50 μg/ml rituximab peptide, irrelevant peptide or buffer. Total samples and supernatant samples were compared via qPCR to determine the percentage of DeNAno displaced from the bead (Figure 5C). Like the streptavidin-specific DeNAno, rituximab-specific 3Rit1 was also released from the target by ligand. This finding further supports the potential application of DeNAno particles as ligand-receptor sensors, whereby a protein-binding event can be reverse-translated into an amplifiable DNA signature.

Finally, 3Rit1 and Bev1 DeNAno and anti-kappa light chain antibody were tested in a protein G sandwich assay to assess DeNAno's ability to overcome the high-dose hook effect (Figure 5D and E). Wash steps were not used until the end of the protocol, as in LFA. First, varying concentrations of rituximab or bevacizumab were pre-incubated with protein G magnetic beads. For anti-kappa antibody samples, mouse IgG was mixed with rituximab and bevacizumab samples that were less than bead-saturating to fill the open protein G binding sites and prevent non-specific antibody binding. Fluorescently-labeled DeNAno particles or anti-kappa antibody were then added (with no washing) and further incubated. After this incubation, beads were washed via magnetic pulldown and analyzed by multimode

microplate reader. The results are graphed as fold-excess free antibody versus fluorescence (Figure 5E). Even in conditions of 100-fold excess free antibody, both DeNAno particles were able to bind their target with no decrease in signal (left y axis). Also, no background staining was observed on irrelevant beads and no binding was observed with non-selected particles (lib-neg). As expected, anti-kappa binding was susceptible to the high-dose hook effect, peaking at 0.1-fold (bevacizumab) or 1-fold (rituximab) and steadily decreasing in fluorescence intensity with increasing free antibody (right y axis). These data parallel the results obtained in the free streptavidin competition and confirm that DeNAno preferentially bind aggregated target over free target.

DISCUSSION

DeNAno particles have previously been selected against cellular targets (1,2). However, characterization of these particles has been limited by the anonymity of the target. Selection of the particles against a well-characterized protein, streptavidin, has allowed for analysis of binding in a variety of conditions, binding competition, particle size required for binding and particle half-life, and has also identified unique features of DeNAno. Two key unique features were observed: (i) DeNAno are displaced from their target by the corresponding ligand and this event can be quantitated by fluorescence or qPCR, (or in the future, high-throughput sequencing) and (ii) DeNAno display a preference for binding to aggregated versus free target and can thus overcome the high-dose hook effect in the presence of 100–1000-fold excess free target (Figure 6A and B).

DeNAno particle displacement from a target by its ligand transforms a protein binding event into a DNA signal, a powerful feature that has potential applicability in high-throughput, highly multiplexed protein or biomarker detection assays. There is increasing need for these types of assays as tissue banks become more expansive, patterns of markers instead of single markers become validated and pharmacologic responses to therapy become more utilized. Current methods, such as mass spectrometry, protein microarrays and bead-based detection assays (e.g., Luminex) exhibit several disadvantages, namely a requirement for specialized and expensive detection equipment, a limit on the degree of multiplexing and/or limited utility for high-throughput screening. A detection assay based on displacement of DeNAno particles would leverage the power and commoditization of sequencing to enable massively parallel analyses that can be inexpensively outsourced to any academic or commercial facility.

In addition to remedying the high-dose hook effect in LFA, DeNAno particles that preferentially bind aggregated target in the presence of free target have potential in biologic detection and targeting. DeNAno particles could be used to identify clusters or aggregates of protein in the presence of large amounts of free (non-aggregated) protein, such as cell-surface antibody in serum-rich environment, fibrin in clots in the presence of free fibrinogen and Alzheimer's-associated amyloid plaques in the presence of amyloid β. The DeNAno likely bind and rapidly release free (individual) targets because only one or a few binding regions are engaged on the particle. It is only when the target is aggregated that a 'velcro-like' interaction can take place–that is, multiple binding sites on the particle binding to multiple targets. This may begin as a 'toehold' of only a few bindings, with the proximity leading to more DeNAno binding site-aggregated target engagements. Thus, when one binding site on the DeNAno detaches, multiple others maintain the DeNAno-aggregated target interaction. Furthermore, due to this proximity, rebinding of unbound DeNAno sites may occur more rapidly than DeNAno/free target.

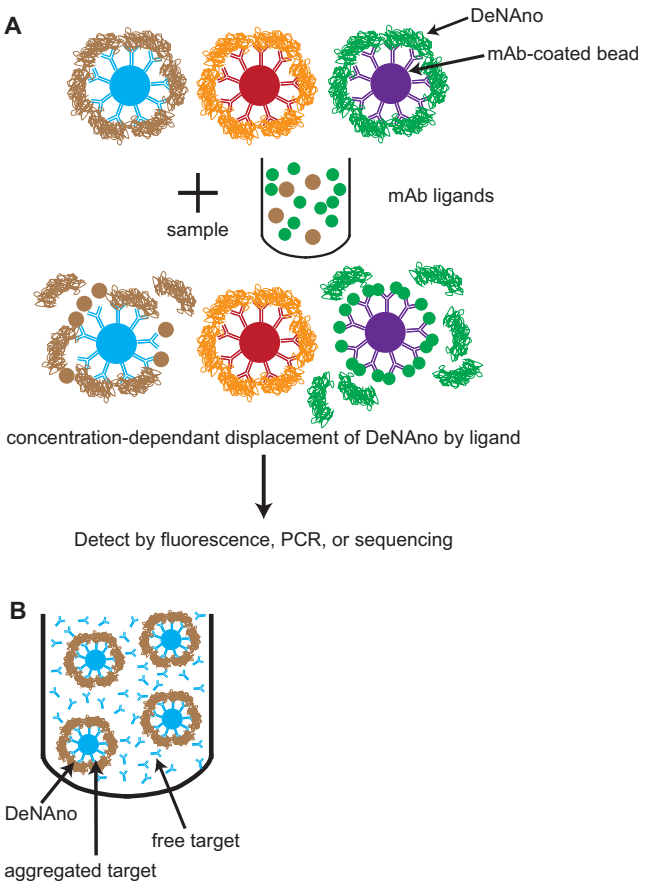

Figure 6. Key features of DeNAno. (**A**) DeNAno bind bead-aggregated target, but are displaced by ligand, transforming a protein-binding event into a DNA signature. (**B**) DeNAno bind aggregated target in the presence of a large excess of free target.

In summary, DeNAno particles hold potential promise as unique and powerful affinity reagents in assays that require massively parallel multiplex detection of binding events, assays which lack an intermediate wash step (e.g. LFA) and other systems where aggregated target must be detected in the presence or absence of free target (e.g. blood clots).

SUPPLEMENTARY DATA

Supplementary Data are available at NAR Online.

ACKNOWLEDGEMENTS

We acknowledge the use of the UCSD Cryo-Electron Microscopy Facility which is supported by NIH grants to Dr Timothy S. Baker and a gift from the Agouron Institute to

UCSD. The authors acknowledge the use of instruments at the Nano and Pico Characterization Lab at the California NanoSystems Institute at UCLA.

FUNDING

National Institutes of Health [R21CA143362 to B.T.M, F32CA180499 to L.E.R., R25CA153915 to A.S., T32EB009380 to J.S.P.]. Funding for open access charge: Abreos Biosciences.

Conflict of interest statement. The DeNAno technology has subsequently been licensed by Abreos Biosciences, a company founded by B.T.M. In addition, L.E.R. has received compensation for consulting services from Abreos Biosciences.

REFERENCES

1. Steiner,J.M., Sartor,M., Sanchez,A.B., Messmer,D., Freed,A., Esener,S. and Messmer,B.T. (2010) DeNAno: selectable deoxyribonucleic acid nanoparticle libraries. *J. Biotechnol.*, **145**, 330–333.
2. Ruff,L.E., Marciniak,J.Y., Sanchez,A.B., Esener,S.C. and Messmer,B.T. (2014) Targeted and reversible cancer cell-binding DNA nanoparticles. *Nanotechnol. Rev.*, **3**, 569–578.
3. Zhao,W., Cui,C.H., Bose,S., Guo,D., Shen,C., Wong,W.P., Halvorsen,K., Farokhzad,O.C., Teo,G.S.L., Phillips,J.A. *et al.* (2012) Bioinspired multivalent DNA network for capture and release of cells. *Proc. Natl. Acad. Sci. U.S.A.*, **109**, 19626–19631.
4. Musumeci,D. and Montesarchio,D. (2012) Polyvalent nucleic acid aptamers and modulation of their activity: a focus on the thrombin binding aptamer. *Pharmacol. Ther.*, **136**, 202–215.
5. Levy-Nissenbaum,E., Radovic-Moreno,A.F., Wang,A.Z., Langer,R. and Farokhzad,O.C. (2008) Nanotechnology and aptamers: applications in drug delivery. *Trends Biotechnol.*, **26**, 442–449.
6. Zhu,J., Huang,H., Dong,S., Ge,L. and Zhang,Y. (2014) Progress in aptamer-mediated drug delivery vehicles for cancer targeting and its implications in addressing chemotherapeutic challenges. *Theranostics*, **4**, 931–944.
7. Tuerk,C. and Gold,L. (1990) Systematic evolution of ligands by exponential enrichment: RNA ligands to bacteriophage T4 DNA polymerase. *Science*, **249**, 505–510.
8. Ellington,A.D. and Szostak,J.W. (1990) In vitro selection of RNA molecules that bind specific ligands. *Nature*, **346**, 818–822.
9. Banerjee,J. and Nilsen-Hamilton,M. (2013) Aptamers: multifunctional molecules for biomedical research. *J. Mol. Med. (Berl).*, **91**, 1333–1342.
10. Hermann,T. and Patel,D.J. (2000) Adaptive recognition by nucleic acid aptamers. *Science*, **287**, 820–825.
11. Sanchez,A.B., Nguyen,T., Dema-Ala,R., Kummel,A.C., Kipps,T.J. and Messmer,B.T. (2010) A general process for the development of peptide-based immunoassays for monoclonal antibodies. *Cancer Chemother. Pharmacol.*, **66**, 919–925.
12. Bailey,T.L., Boden,M., Buske,F.A., Frith,M., Grant,C.E., Clementi,L., Ren,J., Li,W.W. and Noble,W.S. (2009) MEME SUITE: tools for motif discovery and searching. *Nucleic Acids Res.*, **37**, W202–W208.
13. Bing,T., Yang,X., Mei,H., Cao,Z. and Shangguan,D. (2010) Conservative secondary structure motif of streptavidin-binding aptamers generated by different laboratories. *Bioorg. Med. Chem.*, **18**, 1798–1805.
14. Wang,C., Yang,G., Luo,Z. and Ding,H. (2009) In vitro selection of high-affinity DNA aptamers for streptavidin. *Acta Biochim. Biophys. Sin. (Shanghai).*, **41**, 335–340.
15. Bittker,J.A., Le,B.V. and Liu,D.R. (2002) Nucleic acid evolution and minimization by nonhomologous random recombination. *Nat. Biotechnol.*, **20**, 1024–1029.
16. Stoltenburg,R., Reinemann,C. and Strehlitz,B. (2005) FluMag-SELEX as an advantageous method for DNA aptamer selection. *Anal. Bioanal. Chem.*, **383**, 83–91.
17. Chen,H., Meisburger,S.P., Pabit,S.A., Sutton,J.L., Webb,W.W. and Pollack,L. (2012) Ionic strength-dependent persistence lengths of single-stranded RNA and DNA. *Proc. Natl. Acad. Sci. U.S.A.*, **109**, 799–804.
18. Namburi,R., Ponnala,A. and Kancherla,V. (2014) High-dose hook effect. *J. Dr NTR Univ. Health Sci.*, **3**, 5–7.
19. Butch,A.W. (2000) Dilution protocols for detection of hook effects/prozone phenomenon. *Clin. Chem.*, **46**, 1719–1720.
20. Landsteiner,K. (1946) *The Specificity of Serological Reactions*. Harvard University Press, Cambridge.
21. Messmer,B.T., Sullivan,J.J., Chiorazzi,N., Rodman,T.C. and Thaler,D.S. (1999) Two human neonatal IgM antibodies encoded by different variable-region genes bind the same linear peptide: evidence for a stereotyped repertoire of epitope recognition. *J. Immunol.*, **162**, 2184–2192.
22. Parmley,S.F. and Smith,G.P. (1989) Filamentous fusion phage cloning vectors for the study of epitopes and design of vaccines. *Adv. Exp. Med. Biol.*, **251**, 215–218.